SSRG International Journal of Electrical and Electronics Engineering
ISSN: 2348-8379/https://doi.org/10.14445/23488379/IJEEE-V12I12P104

Volume 12 Issue 12, 41-50, December 2025

Original Article

Frequency Regulation of Low Inertia Microgrids by Optimized Tilt Integral Derivative Controller-Based Virtual Inertia Control

P. Narayana Bhaskar[1*], K. Udhayakumar[2]

[1,2]*Department of Electrical and Electronics Engineering, College of Engineering Guindy, Anna University, Chennai, Tamil Nadu, India.*

[*]*Corresponding Author : baski4229@gmail.com*

Received: 03 October 2025 Revised: 05 November 2025 Accepted: 04 December 2025 Published: 27 December 2025

Abstract - *Combining Renewable Energy Sources (RES) with a Micro Grid (MG) lowers system inertia, which makes frequency management more difficult. The idea behind Virtual Inertia Control (VIC) is to use Energy Storage Systems (ESS) to mimic the inertia of a conventional power system. The current work projects an optimized Tilt Integral Derivative (TID) controller for the VIC of low inertia MG with RES using the improved Golf Optimization Algorithm (iGOA). In the beginning, PID controllers are assumed, and the dominance of the iGOA technique is demonstrated over the Golf Optimization Algorithm (GOA) and Sine Cosine Hyperbolic Algorithm (SCHA). In the next stage, Tilt Integral Derivative (TID) controllers are employed, and the TID parameters are tuned by the iGOA method. Simulation results are presented to demonstrate that compared to iGOA optimized PID without VIC and PID with VIC, the proposed TID with VIC scheme achieves superior performance with significantly reduced error metrics across various scenarios, like low-RES penetration, high-RES conditions, variable load with RES penetration, as well as variable load with noise-based RES model.*

Keywords -

1. Introduction

In order to create an autonomous Micro Grid (MG) system, the majority of Renewable Energy Sources (RESs)-based generators, such as solar, wind, and Energy Storage Systems (ESS), are often connected via power electronic devices [1]. Nevertheless, the system inertia significantly decreased as a result of the integration of RES-based generation's inability to provide the inertia characteristics [2]. This can lead to frequency instability and is bad for the system [3]. Instability and a poorer frequency response would result from increased RES penetration [4]. Virtual Inertia Control (VIC) has offered a suitable way to get around this [5, 6]. The VIC concept is applied in Photovoltaic (PV) and wind-integrated systems using ESS in conjunction with RESs. Numerous recent studies on the adaptable inertia and damping scheme have been put forth in the literature [7–10]. The inertia and damping characteristics can be appropriately designed in real-time since inverter-fed Distributed Generators (DGs) are not limited by physical constraints like synchronous generators (SG) [7]. Similar to variable inertia, the droop gain is adjusted as a function of frequency in [8]. A fuzzy secondary controller-based VIC method is used in [9] to reduce MG's frequency deviation. The benefits of high/low inertia are thoroughly discussed in [10], and a concept of distributed VIC is suggested for MGs. D'Arco et al. [11] showed that the VIC system can provide MGs with satisfactory performance under a variety of circumstances. In [12], an algebraic type VIC technique was proposed to enhance the MG frequency response. Engineering applications usually employ PI/PID controllers to achieve control objectives due to their easy implementation.

Traditional PID structures may not offer the requisite system performance if they are coupled with nonlinearity. Conversely, the Tilt Integral Derivative (TID structure has an improvement over the traditional PID. In a TID controller, the tilted proportional term enhances the system stability with increased controller response time. In view of the above, an effort has been made in this work to use the TID controller along with VIC for frequency regulation of an MG. For controller design, usually optimization methods are engaged. The controllers for frequency regulation were designed using a variety of optimization techniques, including enhanced Parasitism Predation Algorithm [13], Sine augmented scaled arithmetic optimization algorithm [14], Genetic Algorithms [15], Chicken Swarm Optimizer [16], Sine Cosine Hyperbolic Algorithm (SCHA) [17], etc. A recently developed optimization method called the Golf Optimization Algorithm

(GOA) is based on the tactical dynamics and player behavior seen in golf [18]. Using test functions, [18] established the superiority of GOA over PSO, GA, GWO, MVO, GSA, WOA, TSA, MPA, and RSA. The no free lunch theorem states that no optimization method is effective for every problem. Innovative methods can be used to complete some activities more effectively.

In the current work, improved GOA (iGOA) is recommended to enhance the potential of GOA, where hyperbolic Sine cosine-based scaling factors are engaged to alter the positions of candidate solutions for a better balance between the exploration and exploitation stages. For virtual inertia control in low-inertia microgrids, existing research primarily uses basic optimization techniques and traditional PID controllers; however, these approaches suffer from high renewable penetration, fluctuating loads, and noisy RES circumstances. Improved optimization methods and sophisticated controllers like TID have not yet been thoroughly investigated for improving frequency stability. As a result, there is a gap in creating a more reliable, precisely calibrated control method that operates consistently in a variety of difficult microgrid circumstances.

The proposed work presents a novel approach by integrating an iGOA with a TID controller for Virtual Inertia Control in low-inertia microgrids, in contrast to previous research that mostly relies on traditional PID controllers optimized using common algorithms like GOA or SCHA. Although PID-based VIC schemes have been the main focus of previous research, they frequently fail to maintain dynamic stability under high renewable penetration, fluctuating loads, and noise-affected RES circumstances. On the other hand, the suggested iGOA-tuned TID controller offers improved tuning precision, quicker reaction times, and increased resilience in a variety of operating conditions. In comparison to current PID-VIC and non-VIC models, this novel combination exhibits improved error reduction and frequency regulation performance, demonstrating the innovation and technical advancement of the current research.

The key features of this article are presented below:

- An improved version of GOA is proposed and compared with GOA and SCHA optimization techniques for PID controller design in the VIC scheme.
- Performance of the iGOA optimized PID without VIC and PID with VIC, TID with VIC scheme is compared to demonstrate the advantage of the proposed TID with VIC scheme.
- A comparative study has been carried out for various scenarios, like low - RES penetration, high-RES conditions, variable load with RES penetration, as well as variable load with a noise-based RES model.

2. Investigated System

Figure 1 shows the diagram of the investigated MG, which includes the Thermal Unit (TU), Solar, Wind, and Energy Storage System (ESS). The ratings are given in the appendix. Nonlinearities like Generator Rate Constraint (GRC) and limiter for TU are considered. The RES's power and load are considered as unrestrained parameters. The controller Gc1(s) controls the reference power setting of the thermal power plant to minimize frequency variations. The parameters of the system are taken from reference [19].

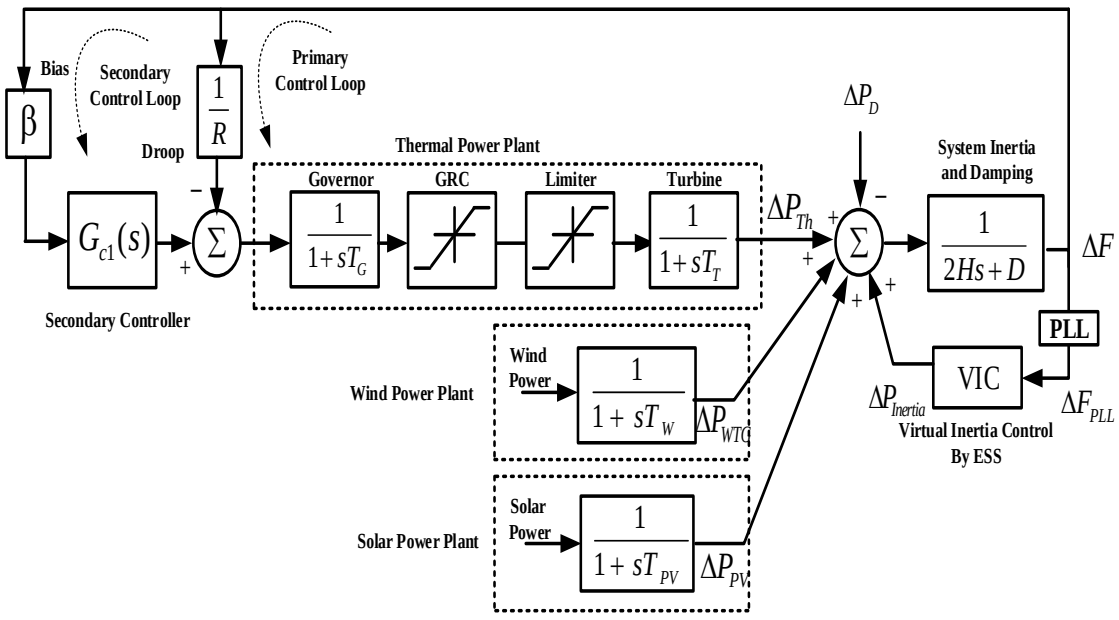

Fig. 1 Investigated MG system

VIC's goal is to provide MG with efficient inertia assistance to sustain system frequency. Figure 2 shows the VIC loop's construction. The controller Gc2(s) controls the inertia power to minimize frequency variations.

A low-pass filter is used to remove noise in order to achieve the properties of ESS. The ESS's output power is restricted by the limiter. The VIC loop's transfer function is [20]:

$$\Delta P_{inertia} = \frac{K_{VI}}{1+T_{VI}s}\left(\frac{d(\Delta f_{PLL})}{dt}\right) \quad (1)$$

Where K_{VI} = gain of VIC, T_{VI} =time constant of VIC, and Δf_{PLL}= output of PLL. The PLL consists of an oscillator, phase detector, and filter, which is adopted from reference [13, 20].

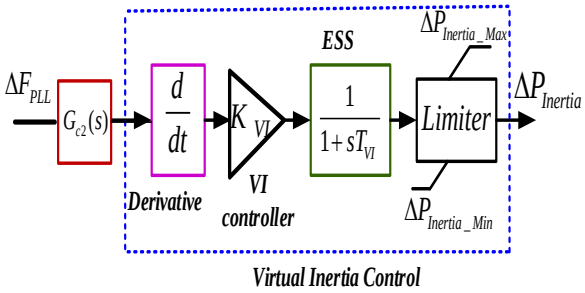

Fig. 2 VIC control loop

3. Proposed Approach

Because of their straightforward design, affordability, and applicability to linear systems, PID structures are typically utilized in control systems. However, nonlinear systems are not necessarily suitable for straightforward PID configurations. As a result, the current study recommends a TID controller, as seen in Figure 3 [21]. With K_P, K_I, and K_D as gains and a tilted component as n, the TID structure is basically a tunable controller.

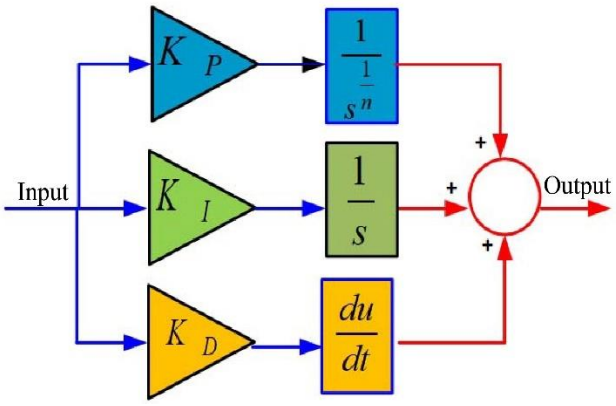

Fig. 3 Configuration of TID controller

$$TF_{TID} = \frac{K_P}{\frac{1}{s^{\frac{1}{n}}}} + \frac{K_I}{s} + K_D s \quad (2)$$

The TID output is:

$$u(t) = K_P \frac{de(\tau)^{-1/n}}{d\tau} + K_I \int_o^t e(\tau)d\tau + K_{D.} \frac{de(\tau)}{d\tau} \quad (3)$$

Where *u(t)* and *e(t)* are the control and error signal.

To decrease Δthe F of the MG, an Integral Squared Error (ISE) measure is considered as the objective function:

$$J = ISE = \int_0^t (\Delta F)^2 dt \quad (4)$$

Where *t* is the time range of the simulation.

4. Overview of Improved iGOA

The GOA is a meticulously structured game-based metaheuristic algorithm that follows exploration and exploitation phases for performing the optimization operation.

The fundamental principles of this activity define the process of hitting a ball from its initial point to the destination hole. Beyond the straightforward exterior principle, the set of laws of the game introduces complexities that increase the level of difficulty in the game. The tactical awareness necessary to put the golf ball in the hole is crucial to the operation. GOA is an innovative metaheuristic algorithm influenced by the strategic approach applied in the Golf game.

The features of the Golf game are intelligently integrated in GOA. The complex movements in the game are outlined, and the conceptual foundations are reinforced by meticulous mathematical modelling. The steps involved in GOA are discussed below.

4.1. Initialization of GOA

Let X be the population matrix, consisting of N GOA members. Each population member X_n Represents a vector of M dimensions which consists of M randomly generated variables, i.e. $X_n = [x_{n,1}, x_{n,2}, \ldots, x_{n,m}, \ldots, x_{n,M}]$. Here, $x_{n,m}$ Represents the mth dimension of nth variable, which is generated randomly in the search space between the predefined lower-bound$L_{B,m}$ and the upper bound $U_{B,m}$. Therefore, the GOA members' random initialization in the population space can be written as

$$X = \begin{bmatrix} X_1 \\ \vdots \\ X_n \\ \vdots \\ X_N \end{bmatrix} = \begin{bmatrix} x_{1,1} & \cdots & x_{1,m} & \cdots & x_{1,M} \\ \vdots & & \vdots & & \vdots \\ x_{n,1} & \cdots & x_{n,m} & \cdots & x_{n,M} \\ \vdots & & \vdots & & \vdots \\ x_{N,1} & \cdots & x_{N,m} & \cdots & x_{N,M} \end{bmatrix} \quad (5)$$

Where $x_{n,m}$ is generated as

$$x_{n,m} = L_{B,m} + r\left(U_{B,m} - L_{B,m}\right) \quad (6)$$

Here, r represents the random value from 0 to 1. After generating all the M variables of the nth member, X_n is implemented on the problem statement to obtain the objective function $F(X_n)$ Which is represented in vector form as

$$F = \begin{bmatrix} F(X_1) \\ \vdots \\ F(X_n) \\ \vdots \\ F(X_N) \end{bmatrix} \quad (7)$$

After evaluating the objective functions for all the members, the best of F is obtained depending on the criteria used in the problem statement (minimization or maximization). Then, the corresponding position in the GOA member is obtained. Both the best objective function and the corresponding position are modified in every iteration.

4.2. Exploration and Exploitation Phase

Each position $x_{n,m}$ In a GOA, a member is updated using the exploration and exploitation phase.

4.2.1. Exploration Phase

The exploration ability known as the global search of the GOA member is indicated by applying the above strategy over the different regions inside the search space. However, when the player hits the ball, there are two possibilities: either it approaches the hole or passes the hole. To indicate these criteria, the variable I is introduced in Eq. (8). The ball approaching the hole and passing the hole are indicated by I=1 and I=2, respectively. Based on the player's best shot, the new location at $(t+1)$th iteration of the GOA member is updated as

$$x_{n,m}(t+1) = x_{n,m}(t) + r\left(x_{best,m} - I x_{n,m}(t)\right) \quad (8)$$

where $x_{best,m}$ Is the best position of the mth variable. Then, $x_{n,m}(t+1)$ is checked for its boundary constraint, and updated as per the expression:

$$x_{n,m}(t+1) = \begin{cases} x_{n,m}(t+1), & L_{B,m} \le x_{n,m}(t+1) \le U_{B,m} \\ L_{B,m}, & x_{n,m}(t+1) < L_{B,m} \\ U_{B,m}, & x_{n,m}(t+1) > U_{B,m} \end{cases} \quad (9)$$

Similarly, all the M variables of nth member are obtained by employing Equations (8) and (9). Then, the objective function $F\left(X_n(t+1)\right)$Is evaluated, which is compared with the objective function $F\left(X_n(t)\right)$ Obtained in the previous iteration. Based on this, the position updationX_n The minimization problem is expressed as

$$X_n = \begin{cases} X_n(t+1), & F\left(X_n(t+1)\right) < F\left(X_n(t)\right) \\ X_n(t), & elsewhere \end{cases} \quad (10)$$

Equation (10) describes that when the fitness of the current location is better than the objective function of the last position, then the last position is replaced by the newly current position.

4.2.2. Exploitation Phase

The careful shot of the player to reach the goal is mathematically modelled by the exploitation phase, which is expressed in Equation (11). This equation denotes the new position of the mth variable of nth member in GOA, which updates based on the problem statement criteria (Maximization and Minimization). Hence, the mathematical expression representing the exploitation strategy is given by:

$$x_{n,m}(t+1) = x_{n,m}(t) + (1-2r)\frac{L_{B,m} + r(U_{B,m} - L_{B,m})}{t} \quad (11)$$

Then, $x_{n,m}(t+1)$ is checked for the boundary constraint as per Equation (9). In this way, all the variables of $X_n(t+1)$ are evaluated, and the corresponding objective function $F\left(X_n(t+1)\right)$ is evaluated.

4.3. Improved GOA (iGOA)

In the premature phases of the GOA algorithm, the best solution is not identified. Consequently, employing huge steps at the start may result in making the solutions past optimal values. Therefore, Scaling Factors (SFs) can be engaged to amend the solutions in the early phases of the GOA. Insertions of SFs alter the positions in the early stages of the GOA process, thus improving the search potential of GOA.

The cyclic function model of hyperbolic sine and cosine functions allocates a solution to change the position to another position. This process can assure better exploitation and exploration potential of GOA.

After finding the positions of $x_{n,m}(t+1)$ After the exploitation strategy using Equation (11), the positions are reorganised using Equation (12). Then, $x_{n,m}(t+1)$ is checked for the boundary constraint as per Equation (5).

$$x_{n,m}(t+1) = x_{n,m}(t+1)/SF \quad (12)$$

Where *SF* is the hyperbolic Sine cosine-based *SF*, which are determined as:

$$SF = \begin{cases} W \sinh\left(2\pi\left(\frac{t}{ITER}\right)\right) & if\ RND \ge 0.5 \\ W \cosh\left(2\pi\left(\frac{t}{ITER}\right)\right) & otherwise \end{cases} \quad (13)$$

For the correct choice of *W*, various values are tried, and it is seen that the finest results are attained when *W* is selected as 10.

5. Results and Discussion

Optimization techniques are engaged for tuning PID/TID parameters for frequency control of the MG system, illustrated in Figure 1. The MATLAB/SIMULINK model is revealed in Figure 4. The system data are provided in the appendix. All the techniques are run for 10 epochs separately, and the finest values, as per the smallest amount of ISE value given by Equation (4), are taken and given in Table 1.

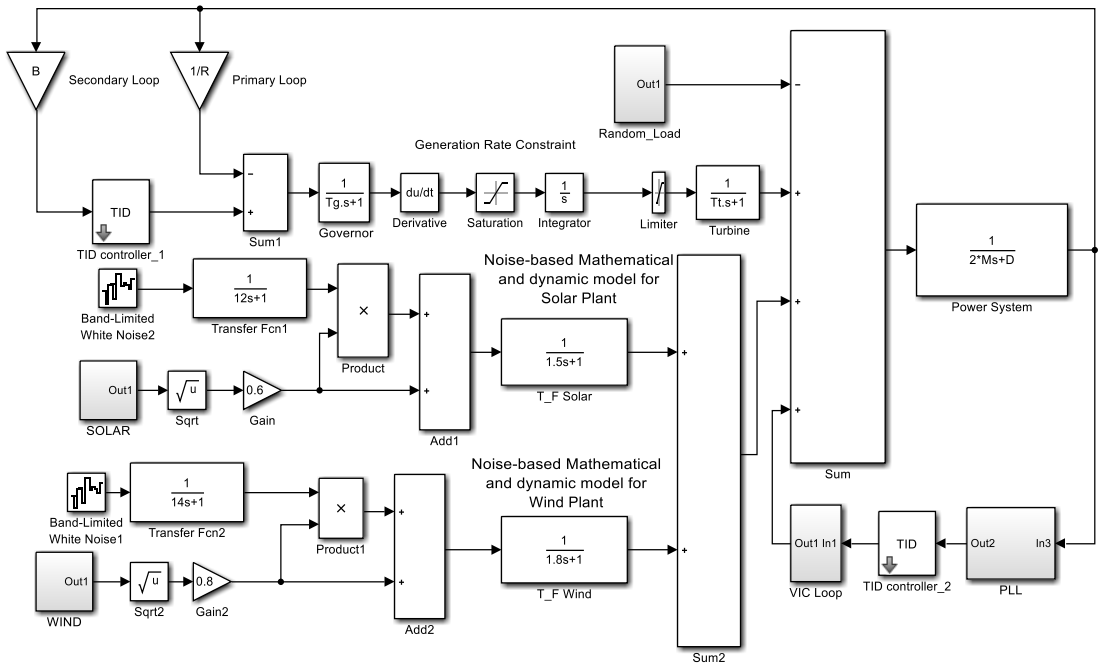

Fig. 4 MATLAB/SIMULINK model of the studied RES Integrated Microgrid with VIC

Table 1. Optimized controller values

Controller	$G_{c1}(s)$				$G_{c2}(s)$				*ISE* Value
	K_P	K_I	K_D	n	K_P	K_I	K_D	n	
SCHA: PID	0.1965	0.8240	1.1729	–	0.7506	1.0155	0.7678	–	0.6444
GOA: PID	0.2965	0.8540	1.1895	–	0.7971	0.4129	0.5670	–	0.6489
iGOA: PID	0.1020	0.7789	0.6958	–	1.0479	0.0047	0.5147	–	0.4546
iGOA: TID	0.6965	1.9585	1.1733	6.7347	1.6420	0.4425	1.6656	3.8617	0.2014

Table 2. Performance with PID tuned using different optimization techniques

Performance	Errors				MO_S	MU_s in (-ve)
	ISE	ITAE	ITSE	IAE		
SCHA	0.6444	10.0622	1.5609	2.2039	0.2263	0.5372
GOA	0.6489	6.8994	1.3522	1.9711	0.1869	0.5567
iGOA	0.4546	4.6152	0.8002	1.5154	0.1849	0.5135

It is obvious from Table 1 that, with a PID controller, a lesser ISE value is found with the iGOA related to GOA and SCHA techniques. Table 1 shows that the ISE value attained with the SCHA method for the PID structure is 0.6444, and the same is 0.6489 with the GOA technique. The ISE value is reduced to 0.4546 with the iGOA-tuned PID controller. The % decrease in ISE value with iGOA related to SCHA and GOA is found to be 29.45% and 29.94% respectively. The frequency deviation response with the PID controller optimized using different optimization techniques is shown in Figure 5. The constant load ΔP_D= 0.15 p.u., wind power ΔP_{WTG}= 0.1 p.u., and solar power ΔP_{PV} = 0.1 p.u. are considered in this case. It is obvious from Figure 5 and Table 1 that for the controller design problem, iGOA outperforms GOA and SCHA techniques. The ISE value is reduced to 0.2014 with the iGOA-tuned TID controller. Hence, for the same technique (iGOA), the % decrease in ISE with the TID controller related to the PID controller is 55.69%. The comparison of time domain parameters (errors, Max. Overshoot (MOs) / Max. Undershoot (MUs)) for the above is provided in Table 2. It is seen that the arithmetical value errors, MOs/MUs with PID, are small with the proposed iGOA technique compared to GOA and SCHA. To assess the time-domain characteristics, different cases are assumed.

5.1. Scenario 1: Low-RES Penetration

In this scenario, constant load ΔP_D= 0.15 p.u., wind power ΔP_{WTG}= 0.1 p.u., and solar power ΔP_{PV} = 0.1 p.u. are considered.

The outcomes with PID (with and without VIC) and TID with VIC are shown in Figures 6-8. For a response without VIC, the second controller $G_{c2}(s)$ is inactive.

It is noticed from Figures 6-8 that, with VIC, the system performance is enhanced. It is also clear from Figure 6 that the response with the TID controller is better than the PID controller.

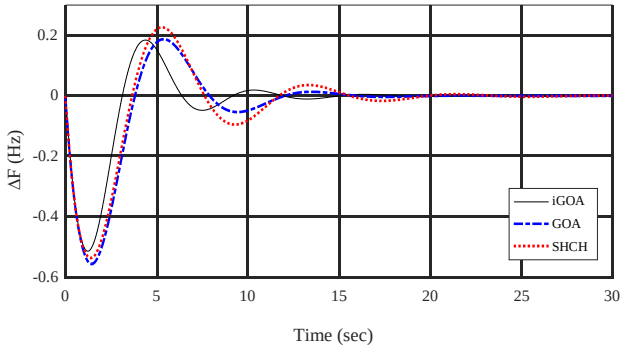

Fig. 5 ΔF Responses with PID controller (different optimization techniques)

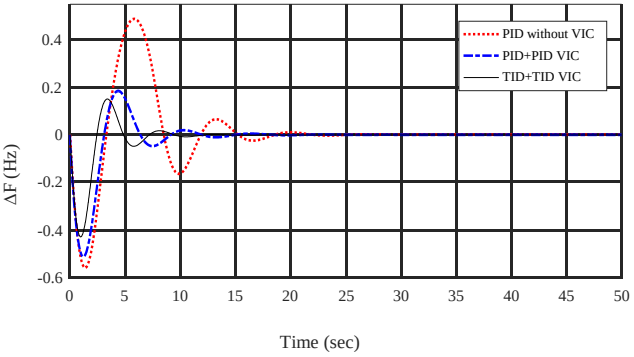

Fig. 6 ΔF Responses with low-RES penetration (scenario 1)

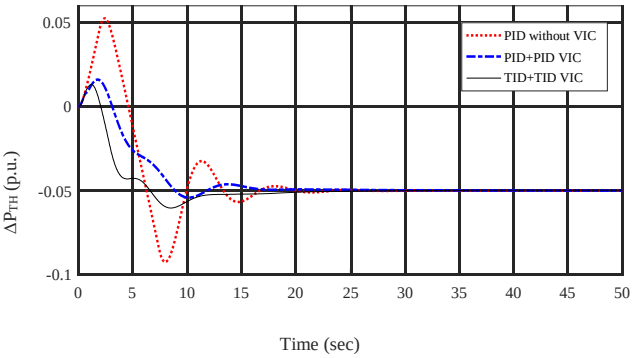

Fig. 7 Thermal power (ΔPTh) responses with low-RES penetration (scenario 1)

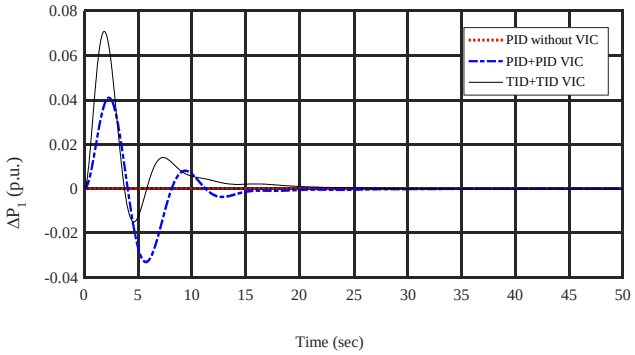

Fig. 8 Inertia Power (ΔP_I) responses with low-RES penetration (scenario 1)

5.2. Scenario 2: High-RES Penetration

In this scenario, constant load ΔP_D= 0.15 p.u., with 50% RES penetration (ΔP_{WTG}= 0.25 p.u. and ΔP_{PV} = 0.25 p.u.), is considered. The response with PID (with and without VIC) and TID with VIC is shown in Figures 9-11.

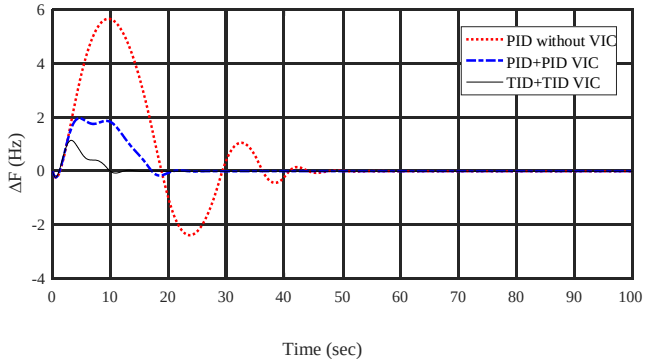

Fig. 9 ΔF Responses with High-RES penetration (scenario 2)

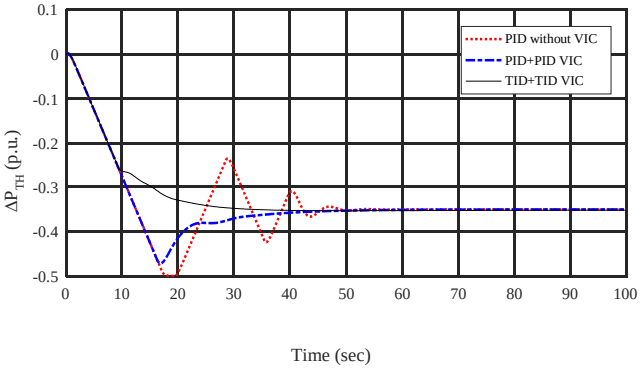

Fig. 10 Thermal power (ΔP_{Th}) responses with high-RES penetration (scenario 2)

It is noticed from Figures 9-11 that, with high-RES penetration, the system performance degrades without VIC.

The results are enhanced considerably with VIC, and the response with TID is better than that of the PID controller.

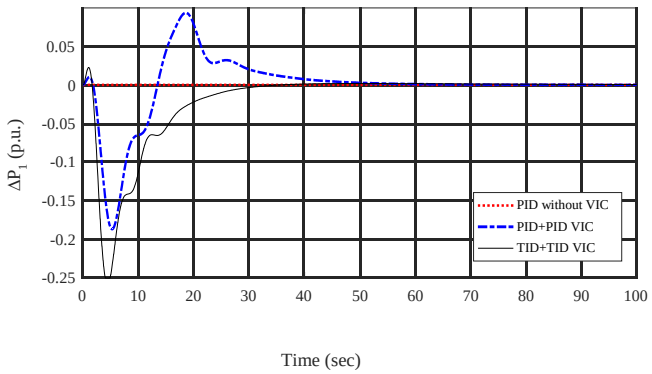

Fig. 11 Inertia Power (ΔP_{Th}) responses with high-RES penetration (scenario 2)

5.3. Scenario 3: Variable Load and RES Penetration

In this scenario, variable load and RES penetration, as shown in Figure 12, are considered, and the system response is revealed in Figures 13-15, from which it is noticed that, with variable load and RES penetration, the system performance degrades without VIC.

Improved results are attained with VIC, and the response with TID is better than that of the PID controller.

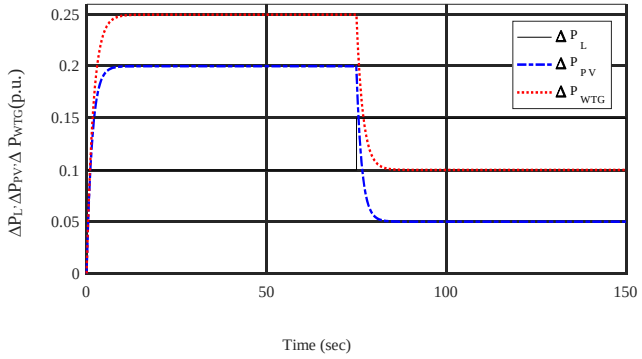

Fig. 12 Variable load and RES pattern (Scenario 3)

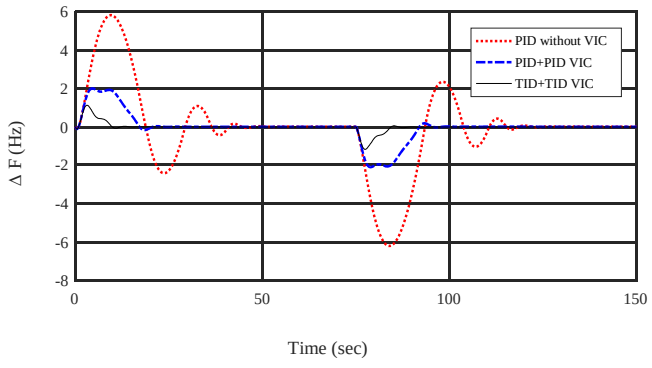

Fig. 13 ΔF Responses with variable load and RES penetration (scenario 3)

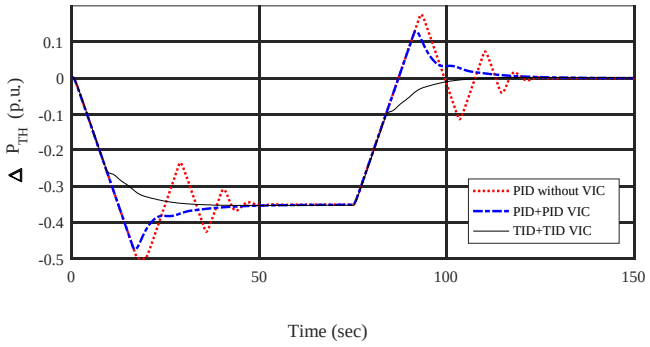

Fig. 14 Thermal power (ΔP_{Th}) responses with variable load and RES penetration (scenario 3)

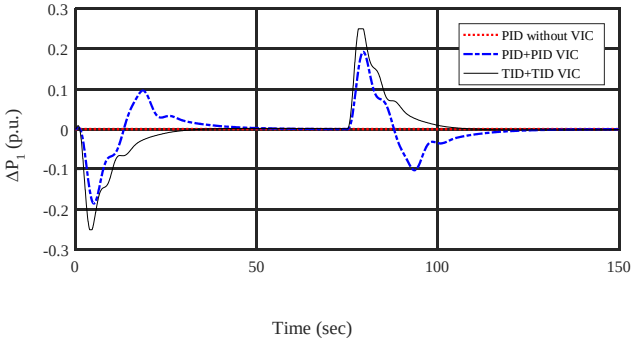

Fig. 15 Inertia Power (ΔP_I) responses with variable load and RES penetration (scenario 3)

5.4. Scenario 4: Variable Load and Noise-Based RES Model

In this scenario, a variable load and noise-based RES model, as shown in Figure 4, is considered.

The variable load and noise-based RES powers are shown in Figure 16.

The system response is shown in Figure 17-19. It is noticed from Figures 17-19 that, with variable load and noise-based RES power penetration, the system performance degrades without VIC, especially during high-RES penetration with low loads (150 sec onwards).

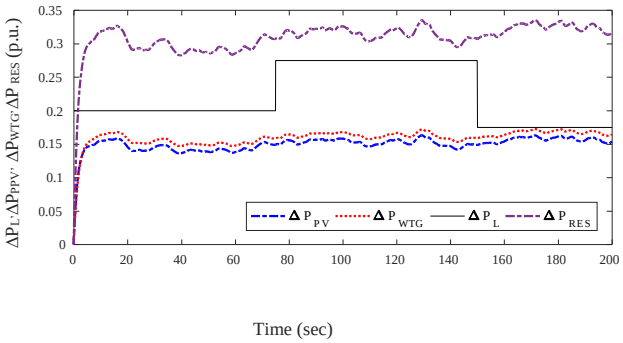

Fig. 16 Variable load and noise-based RES powers (scenario 4)

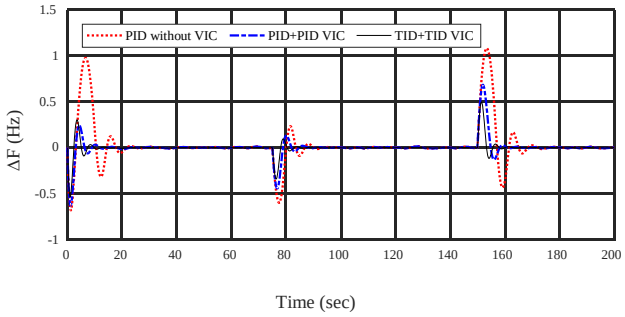

Fig. 17 ΔF Responses with variable load and noise-based RES model (scenario 4)

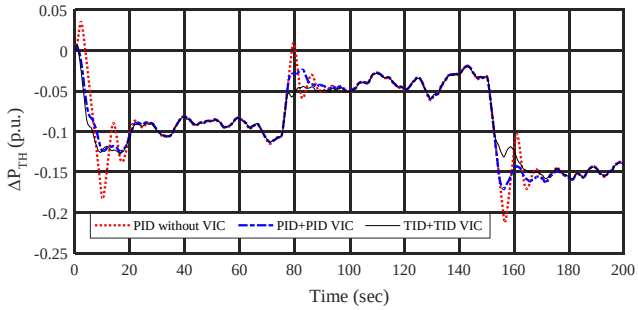

Fig. 18 Thermal Power (ΔP_{Th}) Responses with variable load and noise-based RES model (scenario 4)

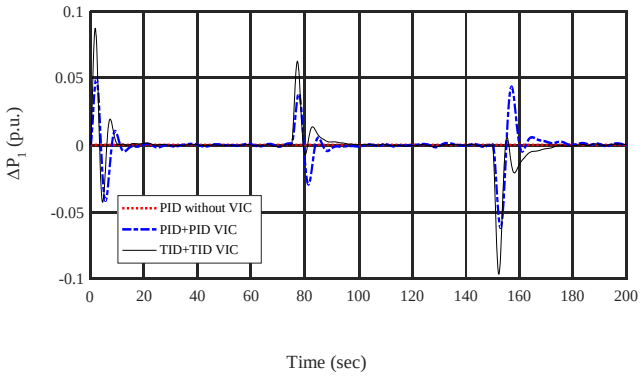

Fig. 19 Inertia Power (ΔP_I) responses with variable load and noise-based RES model (scenario 4)

Improved results are attained with VIC, and the response with TID is better than that of the PID controller.

The comparison of time domain parameters (errors, MOs / MUs) of all scenarios is provided in Table 3.

It is seen that the arithmetical value errors, MOs/MUs with PID, are low with the proposed TID with VIC compared to PID with VIC and PID without VIC.

Table 3. Performance with different controllers for all scenarios

Performance	Errors				MOs	MUs in (-ve)
	ISE	ITAE	ITSE	IAE		
Scenario 1: *Low-RES Penetration*						
PID without VIC	1.2005	18.1888	4.9806	3.3723	0.4874	0.5601
PID with VIC	0.4546	4.6152	0.8002	1.5154	0.1849	0.5135
TID with VIC	0.2443	2.3726	0.3351	0.9832	0.1511	0.4287
Scenario 2: *High-RES Penetration*						
PID without VIC	309.7421	1171.9983	3527.22	83.5075	5.6358	2.3201
PID with VIC	33.4611	179.5680	257.2497	21.5352	1.9702	0.2291
TID with VIC	3.8436	26.4565	15.3094	5.3809	1.1567	0.2186
Scenario 3: *Variable Load and RES Penetration*						
PID without VIC	709.58008	9182.4174	36054.6734	177.529	5.7851	6.1992
PID with VIC	18.1665	904.9032	798.2473	19.7374	1.6261	1.6666
TID with VIC	7.8961	4.632449	339.1944	10.8061	1.1243	1.1569
Scenario 4: *Variable Load and Noise-Based RES Model*						
PID without VIC	10.4676	1413.9551	857.0426	17.5769	1.0818	0.6833
PID with VIC	2.1995	553.4198	199.6254	6.4044	0.6853	0.6341
TID with VIC	1.0479	289.8431	76.4473	3.8683	0.4982	0.5362

6. Conclusion

This work recommends a method for frequency regulation of MG with VIC using optimized controllers. For optimization, the iGOA method is engaged to tune the gains of the TID/PID controller. It is seen that the % decrease in ISE with iGOA related to SCHA and GOA is 29.45% and 29.94% respectively. For the same technique (iGOA), the % decrease in ISE with the TID controller related to the PID controller is 55.69%. Results analysis under various scenarios, like low-RES penetration, high-RES conditions, variable load with RES penetration, as well as variable load with noise-based RES model, indicates that significantly improved results are attained with VIC, and the response with the TID controller is better than the PID controller. It is also noticed that, with high-RES penetration, the system performance degrades without VIC. As future work, VIC control in multi-area systems may be investigated.

Acknowledgments

The supervisor's direction and continuous support throughout this research are greatly appreciated by the author.

References

[1] Nagaraju Pogaku, Milan Prodanovic, and Timothy C. Green, "Modeling, Analysis and Testing of Autonomous Operation of an Inverter-Based Microgrid," *IEEE Transactions on Power Electronics*, vol. 22, no. 2, pp. 613-625, 2007. [CrossRef] [Google Scholar] [Publisher Link]

[2] Karel De Brabandere et al., "A Voltage and Frequency Droop Control Method for Parallel Inverters," *IEEE Transactions on Power Electronics*, vol. 22, no. 4, pp. 1107-1115, 2007. [CrossRef] [Google Scholar] [Publisher Link]

[3] Hasan Alrajhi Alsiraji, and Ramadan El-Shatshat, "Comprehensive Assessment of Virtual Synchronous Machine-Based Voltage Source Converter Controllers," *IET Generation, Transmission & Distribution*, vol. 11, no. 7, pp. 1762-1769, 2017. [CrossRef] [Google Scholar] [Publisher Link]

[4] Jia Liu et al., "Enhanced Virtual Synchronous Generator Control for Parallel Inverters in Microgrids," *IEEE Transactions on Smart Grid*, vol. 8, no. 5, pp. 2268-2277, 2017. [CrossRef] [Google Scholar] [Publisher Link]

[5] Won-Sang Im et al., "Distributed Virtual Inertia-Based Control of Multiple Photovoltaic Systems in Autonomous Microgrid," *IEEE/CAA Journal of Automatica Sinica*, vol. 4, no. 3, pp. 512-519, 2017. [CrossRef] [Google Scholar] [Publisher Link]

[6] Yiwei Ma et al., "Virtual Synchronous Generator Control of Full Converter Wind Turbines with Short-Term Energy Storage," *IEEE Transactions on Industrial Electronics*, vol. 64, no. 11, pp. 8821-8831, 2017. [CrossRef] [Google Scholar] [Publisher Link]

[7] Miguel A. Torres L. et al., "Self-Tuning Virtual Synchronous Machine: A Control Strategy for Energy Storage Systems to Support Dynamic Frequency Control," *IEEE Transactions on Energy Conversion*, vol. 29, no. 4, pp. 833-840, 2014. [CrossRef] [Google Scholar] [Publisher Link]

[8] Nimish Soni et al., "Improvement of Transient Response in Microgrids using Virtual Inertia," *IEEE Transactions on Power Delivery*, vol. 28, no. 3, pp. 1830-1838, 2013. [CrossRef] [Google Scholar] [Publisher Link]

[9] Chowdhury Andalib-Bin-Karim, Xiaodong Liang, and Huaguang Zhang, "Fuzzy-Secondary-Controller-Based Virtual Synchronous Generator Control Scheme for Interfacing Inverters of Renewable Distributed Generation in Microgrids," *IEEE Transactions on Industry Applications*, vol. 54, no. 2, pp. 1047-1061, 2018. [CrossRef] [Google Scholar] [Publisher Link]

[10] Jingyang Fang et al., "Distributed Power System Virtual Inertia Implemented by Grid-Connected Power Converters," *IEEE Transactions on Power Electronics*, vol. 33, no. 10, pp. 8488-8499, 2018. [CrossRef] [Google Scholar] [Publisher Link]

[11] Salvatore D'Arco, Jon Are Suul, and Olav B. Fosso, "A Virtual Synchronous Machine Implementation for Distributed Control of Power Converters in SmartGrids," *Electric Power Systems Research*, vol. 122, no. 1, pp. 180-197, 2015. [CrossRef] [Google Scholar] [Publisher Link]

[12] Yuko Hirase et al., "A Grid-Connected Inverter with Virtual Synchronous Generator Model of Algebraic Type," *Electrical Engineering in Japan*, vol. 184, no. 4, pp. 10-21, 2013. [CrossRef] [Google Scholar] [Publisher Link]

[13] Rajendra Kumar Khadanga et al., "An Improved Parasitism Predation Algorithm for Frequency Regulation of a Virtual Inertia Control-Based AC Microgrid," *Energy Sources, Part A: Recovery, Utilization, and Environmental Effects*, vol. 44, no. 1, pp. 1660-1677, 2022. [CrossRef] [Google Scholar] [Publisher Link]

[14] Rajendra Kumar Khadanga et al., "Sine Augmented Scaled Arithmetic Optimization Algorithm for Frequency Regulation of a Virtual Inertia Control based Microgrid," *ISA Transactions*, vol. 138, pp. 534-545, 2023. [CrossRef] [Google Scholar] [Publisher Link]

[15] Rajasi Mandal, and Kalyan Chatterjee, "Virtual Inertia Emulation and RoCoF Control of a Microgrid with High Renewable Power Penetration," *Electric Power Systems Research*, vol. 194, 2021. [CrossRef] [Google Scholar] [Publisher Link]

[16] Ahmed M. Othman, and Attia A. El-Fergany, "Adaptive Virtual-Inertia Control and Chicken Swarm Optimizer for Frequency Stability in Powergrids Penetrated by Renewable Energy Sources," *Neural Computing and Applications*, vol. 33, no. 7, pp. 2905-2918, 2021. [CrossRef] [Google Scholar] [Publisher Link]

[17] Jianfu Bai et al., "A Sinhcosh Optimizer," *Knowledge-Based Systems*, vol. 282, 2023. [CrossRef] [Google Scholar] [Publisher Link]

[18] Zeinab Montazeri et al., "Golf Optimization Algorithm: A New Game-Based Metaheuristic Algorithm and Its Application to Energy Commitment Problem Considering Resilience," *Biomimetics*, vol. 8, no. 5, pp. 1-37, 2023. [CrossRef] [Google Scholar] [Publisher Link]

[19] Mohammad Hossein Norouzi et al., "Learning-based Virtual Inertia Control of an Islanded Microgrid with High Participation of Renewable Energy Resources," *IEEE Systems Journal*, vol. 18, no. 2, pp. 1-10, 2024. [CrossRef] [Google Scholar] [Publisher Link]

[20] Thongchart Kerdphol et al., "Robust Virtual Inertia Control of a Low Inertia Microgrid Considering Frequency Measurement Effects," *IEEE Access*, vol. 7, pp. 57550-57560, 2019. [CrossRef] [Google Scholar] [Publisher Link]

[21] Rajendra Kumar Khadanga et al., "Design and Analysis of Tilt Integral Derivative Controller for Frequency Control and in an Islanded Micro-Grid: A Novel Hybrid Dragonfly and Pattern Search Algorithm Approach," *Arabian Journal of Science and Engineering*, vol. 43, no. 6, pp.3103-3114, 2018. [CrossRef] [Google Scholar] [Publisher Link]

Appendix 1

Ratings: Thermal unit=12 MW, ESS=4 MW, Solar unit=6 MW, Wind unit =15 MW. Tg =0.1 s, Tt=0.4 s, TVI =0.4 s, β =1 p.u.MW/Hz; R =2.4 Hz/p.u.MW; D =0.015 p.u.MW/Hz, H =0.083 p.u.MW s; TWT =1.5 s, TPV =1.85 s, VU/VL =±0.5, ESS limit = ±0.25 p.u., KVT =0.8.